

Stable and Transparent Superhydrophobic Nanoparticle Films

Xing Yi Ling,[†] In Yee Phang,[‡] G. Julius Vancso,[‡] Jurriaan Huskens,^{*,†} and David N. Reinhoudt^{*,†}

Molecular Nanofabrication Group, MESA+ Institute for Nanotechnology, University of Twente, P.O. Box 217, 7500 AE, Enschede, The Netherlands, and Materials Science and Technology of Polymers, MESA+ Institute for Nanotechnology, University of Twente, P.O. Box 217, 7500 AE, Enschede, The Netherlands

Received December 10, 2008

A superhydrophobic surface with a static water contact angle (θ_w) > 150° was created by a simple “dip-coating” method of 60-nm SiO₂ nanoparticles onto an amine-terminated (NH₂) self-assembled monolayer (SAM) glass/silicon oxide substrate, followed by chemical vapor deposition of a fluorinated adsorbate. For comparison, a close-packed nanoparticle film, formed by convective assembly, gave $\theta_w \sim 120^\circ$. The stability of the superhydrophobic coating was enhanced by sintering of the nanoparticles in an O₂ environment at high temperature (1100 °C). A sliding angle of <5° indicated the self-cleaning properties of the surface. The dip-coating method can be applied to glass substrates to prepare surfaces that are superhydrophobic and transparent.

Introduction

Self-cleaning superhydrophobic surfaces might have an important applicability on our day-to-day life.¹ Superhydrophobic surfaces of natural objects, such as the lotus leaf,² the namib desert beetle,³ the gecko,⁴ and water strider,^{5,6} have revealed that superhydrophobic characteristics are achieved by combining micro and nanoroughness with a hydrophobic coating of low surface energy.^{7–10}

Artificial superhydrophobic surfaces are generally prepared by a two-step method.¹¹ First, a surface with micro- or nanosized roughness is created by lithography or by deposition of a micro- or nanomaterials.¹² Subsequently, molecules with a low surface energy are deposited to provide water-repelling properties. Photolithography has been extensively used to create surfaces with micro- or nanosized pillars with different dimensions and aspect ratios to mimic natural submicrometer features that enhance the water-repelling properties.^{13,14} Deposition of micro or nanomaterials, such as silanes, polymers, and nanoparticles, has also been extensively studied owing to its relatively cheap fabrication costs.^{15–18} McCarthy et al. have created nanofiber networks by a combination of mixtures of silanes, which resulted in an excellent hydrophobic surface.¹⁶ Rubner et al. have

fabricated a honeycomb-like polyelectrolyte multilayer surface coated with silica nanoparticles and semifluorinated silanes, which showed superhydrophobic properties after extended immersion in water.¹⁷ The hydrophobic characteristics of a layer of silica particles deposited by the Langmuir–Blodgett technique, functionalized with alkylsilanes to yield a static contact angle of 130°. ¹⁹ The deposition of hydrophobic polyaniline microspheres on a glass surface by a template-free method also resulted in hydrophobic surface.²⁰ Recently, our group reported the conversion of a superhydrophobic silica nanoparticle surface to an ultraphobic surface by a two-scale roughness.²¹

Here we report a simple method to create a superhydrophobic surface by combination of nanoparticle deposition and fluorosilane functionalization on glass/silicon oxide substrates. Our method is lithography-free, low-cost, and can be applied over a large area. Unfunctionalized SiO₂ nanoparticles are assembled onto a self-assembled monolayer (SAM)-covered substrate by dipping the substrate into the nanoparticle solution, followed by 1H,1H,2H,2H-perfluorodecyltriethoxysilane (PFTS) gas-phase deposition. The hydrophobicity of the sample is compared to that of a close-packed nanoparticle film formed by convective assembly. The mechanical stability of the dip-coated nanoparticle film is tested before and after sintering. We also describe the formation of a transparent superhydrophobic coating based on this method.

Experimental Section

Chemicals. Tetraethyl orthosilicate (Sigma Aldrich), 3-aminopropyl triethoxysilane (APTES), PFTS (ABCR), and adhesive tape (3M, Minnesota) were obtained from commercial sources. Milli-Q water with a resistivity greater than 18 M Ω ·cm was used in all experiments.

Preparation of Bare Silica Nanoparticles. Bare silica nanoparticles were synthesized following a literature procedure.²² Briefly, 3.8 mL of tetraethyl orthosilicate was added to a flask containing

* Corresponding author. E-mail: J.Huskens@tnw.utwente.nl (J.H.); D.N.Reinhoudt@tnw.utwente.nl (D.N.R.).

[†] Molecular Nanofabrication Group.

[‡] Materials Science and Technology of Polymers.

(1) Nakajima, A.; Hashimoto, K.; Watanabe, T.; Takai, K.; Yamauchi, G.; Fujishima, A. *Langmuir* **2000**, *16*, 7044.

(2) Barthlott, W.; Neinhuis, C. *Planta* **1997**, *202*, 1.

(3) Zhai, L.; Berg, M. C.; Cebeci, F. C.; Kim, Y.; Milwid, J. M.; Rubner, M. F.; Cohen, R. E. *Nano Lett.* **2006**, *6*, 1213.

(4) Kustandi, T. S.; Samper, V. D.; Yi, D. K.; Ng, W. S.; Neuzil, P.; Sun, W. *Adv. Funct. Mater.* **2007**, *17*, 2211.

(5) Gao, X.; Jiang, L. *Nature* **2004**, *432*, 36.

(6) Shi, F.; Niu, J.; Liu, J. L.; Liu, F.; Wang, Z. Q.; Feng, X. Q.; Zhang, X. *Adv. Mater.* **2007**, *19*, 2257.

(7) Wenzel, R. N. *Ind. Eng. Chem.* **1936**, *28*, 988.

(8) Cassie, A. B. N.; Baxter, S. *Trans. Faraday Soc.* **1944**, *40*, 546.

(9) Oner, D.; McCarthy, T. J. *Langmuir* **2000**, *16*, 7777.

(10) Callies, M.; Quere, D. *Soft Matter* **2005**, *1*, 55.

(11) Li, X. M.; Reinhoudt, D.; Crego-Calama, M. *Chem. Soc. Rev.* **2007**, *36*, 1350.

(12) Tserepi, A. D.; Vlachopoulou, M. E.; Gogolides, E. *Nanotechnology* **2006**, *17*, 3977.

(13) Martinez, E.; Seunarine, K.; Morgan, H.; Gadegaard, N.; Wilkinson, C. D. W.; Riehle, M. O. *Nano Lett.* **2005**, *5*, 2097.

(14) Zhu, L.; Feng, Y. Y.; Ye, X. Y.; Zhou, Z. Y. *Sens. Actuators, A* **2006**, *130*, 595.

(15) Soeno, T.; Inokuchi, K.; Shiratori, S. *Appl. Surf. Sci.* **2004**, *237*, 543.

(16) Gao, L. C.; McCarthy, T. J. *J. Am. Chem. Soc.* **2006**, *128*, 9052.

(17) Zhai, L.; Cebeci, F. C.; Cohen, R. E.; Rubner, M. F. *Nano Lett.* **2004**, *4*, 1349.

(18) Ofir, Y.; Samanta, B.; Arumugam, P.; Rotello, V. M. *Adv. Mater.* **2007**, *19*, 4075.

(19) Tsai, P. S.; Yang, Y. M.; Lee, Y. L. *Langmuir* **2006**, *22*, 5660.

(20) Ding, H. J.; Zhu, C. J.; Zhou, Z. M.; Wan, M. X.; Wei, Y. *Macromol. Rapid Commun.* **2006**, *27*, 1029.

(21) Li, X. M.; He, T.; Crego-Calama, M.; Reinhoudt, D. N. *Langmuir* **2008**, *24*, 8008.

(22) Ling, X. Y.; Reinhoudt, D. N.; Huskens, J. *Langmuir* **2006**, *22*, 8777.

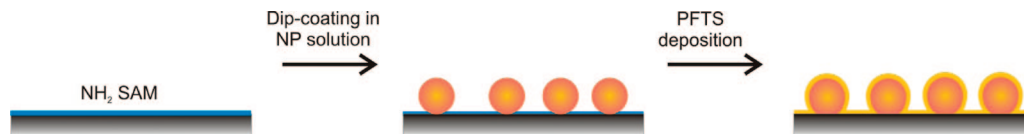


Figure 1. Scheme of creating a superhydrophobic surface via the assembly of nanoparticles onto the substrate, followed by deposition of a fluorinated silane.

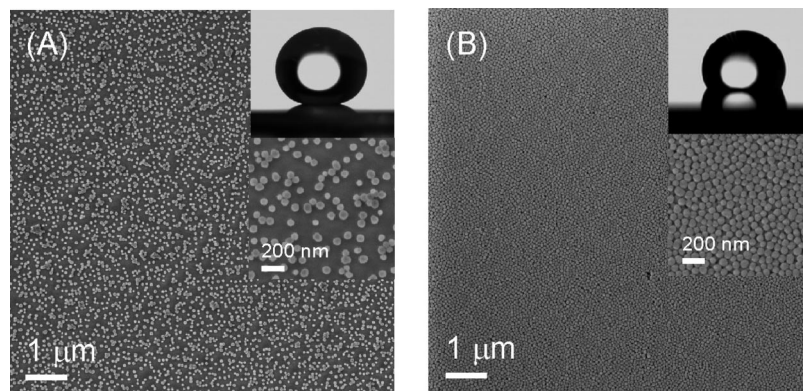


Figure 2. SEM images of the dip-coated (A) and convectively assembled (B) nanoparticle films. The insets show a water droplet on each of the nanoparticle films after PFTS functionalization and zoom-in SEM images.

5.7 mL of concentrated ammoniumhydroxide and 114 mL of ethanol while stirring. The stirring was continued overnight. This resulted in the formation of approximately 60 nm silica nanoparticles, as characterized by scanning electron microscopy (SEM).

Substrate and Monolayer Preparation. Silicon substrates were cleaned by immersion in piranha solution (conc. H_2SO_4 and 33% H_2O_2 in a 3:1 volume ratio; **Warning! Piranha should be handled with caution; it can detonate unexpectedly!**) for 15 min to form a SiO_2 layer on the surface. The substrates were then sonicated in Milli-Q water and ethanol for 1 min, and dried with a stream of N_2 . Amino-terminated SAMs (NH_2 -SAMs) were obtained by gas-phase evaporation of APTES in a desiccator under vacuum for several hours, and then carefully rinsed with ethanol and Milli-Q water.

Preparation of Superhydrophobic Surfaces. A silica nanoparticle aqueous solution (0.6 mg/mL, pH 7) was sonicated for 15 min before use. An amino SAM-coated glass/silicon oxide substrate was dipped into the nanoparticle solution for 10 min, and subsequently rinsed with water thoroughly. For another sample, the SiO_2 nanoparticles were assembled onto an amino SAM by capillary-assisted assembly from the silica nanoparticle suspension at a constant speed of $1 \mu\text{m/s}$.^{23,24} The substrate layers were ultrasonicated for 20 s, rinsed with pH 2 water, and Milli-Q water, and gently blown dry with N_2 . The substrates were subsequently exposed to PFTS by gas-phase evaporation in a desiccator under vacuum for at least 5 h. Sintering of the nanoparticles was carried out in a furnace (Amtech Tempress omega junior) at $900\text{--}1100^\circ\text{C}$, for 30–120 min in an O_2 atmosphere.

Analysis. Contact angles were measured on a Krüss G10 contact angle measuring instrument, equipped with a CCD camera. Static water contact angles were measured with a $4 \mu\text{L}$ Milli-Q water droplet, and advancing and receding contact angles were determined automatically during growth and shrinkage of the droplet of Milli-Q water by a drop shape analysis routine. Five measurements were made on each surface. All SEM images were taken with a HR-LEO 1550 FEF SEM. Ultraviolet–visible (UV–vis) spectra were recorded on a Varian Cary 300 Bio instrument in double-beam mode, using an uncovered glass slide as a reference. The glass slide was placed perpendicular to the beam to maintain the same positioning during each measurement. AFM measurements were carried out with a Dimension D3100 using a NanoScope IV controller equipped with a hybrid 153 scanner (Veeco/Digital Instruments (DI), Santa Barbara, CA) under ambient conditions. Silicon cantilevers from Nanosensors (Nanosensors, Wetzlar, Germany) were used for intermittent contact (tapping) mode operation.

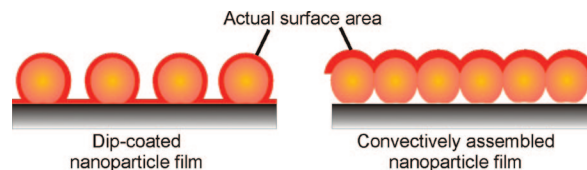


Figure 3. Schematic surface areas of the dip-coated and convectively assembled nanoparticle films.

Results and Discussion

A superhydrophobic surface was created by the subsequent introduction of roughness via a dip-coating deposition of nanoparticles, and hydrophobicity by the deposition of a fluorinated monolayer. Electrostatic interactions between a charged surface and oppositely charged nanoparticles were employed to direct the deposition of the nanoparticles on the surface. As shown in Figure 1, a piranha-cleaned glass/silicon oxide surface was functionalized with APTES via chemical vapor deposition to form an NH_2 -SAM. The substrate was dipped into a solution of unfunctionalized SiO_2 nanoparticles²² (60 nm in diameter) for 10 min, followed by rinsing with water. For comparison, a nanoparticle film was also formed using convective assembly.²⁵ Subsequently, PFTS was chemically deposited on both substrates via chemical vapor deposition.

The SEM image (Figure 2A) of a typical nanoparticle film obtained by dip-coating shows a moderately dense coverage of nanoparticles adsorbed on the NH_2 -SAM distributed across the surface in a noncontinuous and scattered manner. No aggregates of nanoparticles are observed, likely as a result of electrostatic repulsion between the nanoparticles. The convectively assembled nanoparticle film was denser and close-packed (Figure 2B). It is known that convective assembly typically leads to very dense layers as a result of capillary forces arising upon solvent evaporation during the assembly process.²⁵

(23) Maury, P.; Péter, M.; Crespo-Biel, O.; Ling, X. Y.; Reinhoudt, D. N.; Huskens, J. *Nanotechnology* **2007**, *18*, 044007.

(24) Ling, X. Y.; Phang, I. Y.; Reinhoudt, D. N.; Vancso, G. J.; Huskens, J. *Int. J. Mol. Sci.* **2008**, *9*, 486.

(25) Ling, X. Y.; Malaquin, L.; Reinhoudt, D. N.; Wolf, H.; Huskens, J. *Langmuir* **2007**, *23*, 9990.

Table 1. Static and Dynamic Water Contact Angles and AFM-Measured rms Roughnesses of Surfaces Deposited with Nanoparticles

substrate	static contact angle (°)	advancing contact angle (°)	receding contact angle (°)	average rms roughness (nm)
PFTS SAM	110 ± 3	124 ± 3	80 ± 3	1
dip-coated nanoparticle film	<20	<20	<20	26
dip-coated nanoparticle film + deposition of PFTS	152 ± 2	155 ± 2	130 ± 2	26
convectively assembled nanoparticle film + deposition of PFTS	120 ± 2	125 ± 2	70 ± 2	6

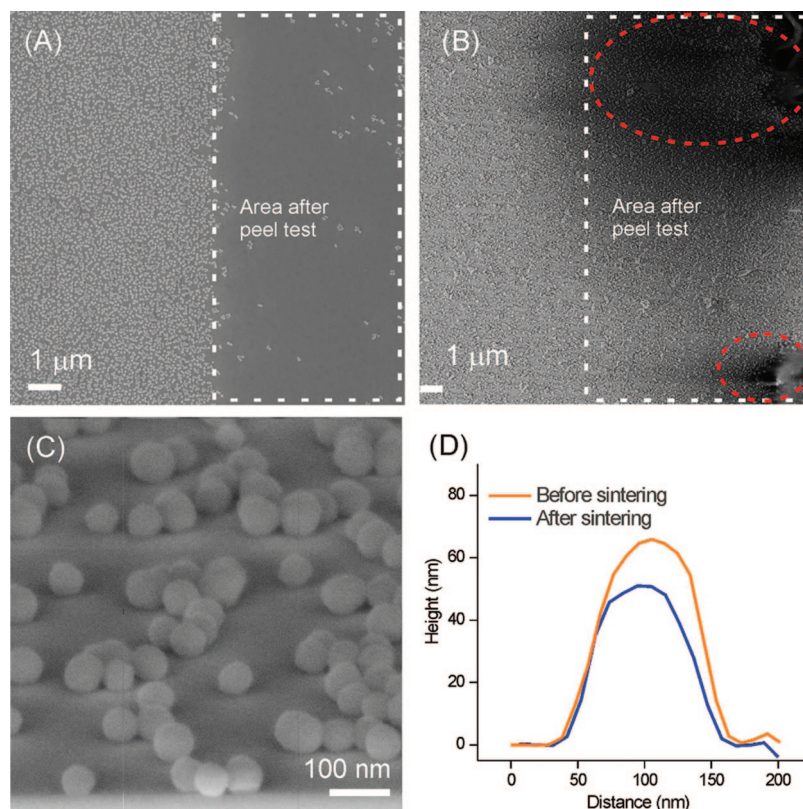


Figure 4. SEM images of the peel test on dip-coated nanoparticle films before (A) and after a sintering process (B); white boxes indicate the areas after peel tests, while red-dot ellipsoids show the area where scotch tape adhesives remained on the substrate after the test. (C) Titled SEM image of the nanoparticles after sintering, and (D) averaged height profiles of the nanoparticles before and after sintering (as measured by AFM).

The static, advancing (θ_a), and receding (θ_r) water contact angles of the PFTS-functionalized SAMs on silicon substrates, and the dip-coated and convectively assembled nanoparticle films were measured before and after chemical vapor deposition of PFTS (Table 1). On substrates without nanoparticles, the PFTS-functionalized SAMs exhibited a static water contact angle of 110°, with $\theta_a/\theta_r = 124^\circ/80^\circ$. The formation of a hydrophobic surface on these substrates indicated that PFTS, owing to its low surface energy, is a suitable candidate to induce superhydrophobicity. Before and after PFTS deposition, the dip-coated nanoparticle film showed static water contact angles of <20° and 152°, respectively, with $\theta_a/\theta_r = 155^\circ/130^\circ$ in the latter case. The drastic change of the contact angle from hydrophilic to superhydrophobic on the dip-coated nanoparticle film indicated that a fluorinated SAM was formed on the surface of nanoparticles. Compared to a flat PFTS SAM substrate, the dip-coated and silanized nanoparticle films have achieved superhydrophobic properties ($\theta_w > 150^\circ$), which is attributed to the combination of surface roughness and hydrophobicity.¹¹ The convectively assembled nanoparticle film, after PFTS functionalization, showed a contact angle of only 120°, with $\theta_a/\theta_r = 125^\circ/70^\circ$ (inset of Figure 2B). This means that the nanoparticle coverage is important to render the substrate superhydrophobic. Sliding angle measurement of the superhydrophobic surface showed that a water droplet

rolls off the surface already at a tilt angle of <5°, indicating that this superhydrophobic surface possesses self-cleaning properties.

The Wenzel equation, $\cos \theta_w = r \times \cos \theta_y$ was applied to explain the difference in wettability between the dip-coated and convectively assembled substrates.^{7,26,27} The measured contact angle is θ_w , θ_y is Young's contact angle, and the roughness ratio, i.e., the ratio between the actual and projected surface area, is r . The actual surface area of a nanoparticle on a surface is ~4 times higher than the projected surface area.²⁸ On the basis of the Wenzel equation, the PFTS-functionalized dip-coated and convectively assembled nanoparticle films yielded roughness factors of 2.53 and 1.46 with respect to a PFTS film, respectively. Atomic force microscopy (AFM) height images can be used to determine the root-mean-square (rms) roughness of the nanoparticle films. The rms roughness describes the rms value of the surface height relative to the center place.²⁹ It is therefore influenced by different factors, e.g., the sharpness of the AFM tip, scan size of the AFM image, the size of the nanoparticles,

(26) Marmur, A. *Soft Matter* **2006**, *2*, 12.

(27) The size of the water droplet during contact angle measurement is at least 2–3 orders of magnitude larger than the roughness of the sample. Hence, the Wenzel equation is applicable here.

(28) The actual surface area of a 60-nm SiO₂ nanoparticle is $\sim 11 \times 10^3$ nm², whereas its projected surface area is $\sim 2.8 \times 10^3$ nm².

(29) Smith, P. F.; Chun, I.; Liu, G.; Dimitrievich, D.; Rasburn, J.; Vancso, G. J. *Polym. Eng. Sci.* **1996**, *36*, 2129.

and the packing density of the nanoparticle film. In our case, the first three variables can be excluded to contribute to the difference in roughness, because all AFM images were measured at a scan size of $2\ \mu\text{m} \times 2\ \mu\text{m}$, and the AFM tips and the nanoparticles used are the same. The nanoparticle film prepared by dip-coating exhibited an average roughness of 26 nm, whereas the average roughness of a sample by convective assembly was 6 nm (Table 1). Both the roughness factors, as assessed by Wenzel equation, and the average roughness as measured by AFM, indicate that the difference in roughness originates from the difference in packing of the nanoparticle films (Figure 3). The dip-coating method allows attachment of nanoparticles in a random and scattered manner, which results in spacing between the nanoparticles. This spacing creates a larger surface area on the film, and thus more pinning points for water repellency (Figure 3). The convectively assembled nanoparticle film has no spacing between adjacent nanoparticles, resulting in a smaller exposed surface area when compared to the dip-coated film. Control over the surface coverage, as achieved by dip-coating, is thus essential for obtaining a superhydrophobic surface.

For potential commercial application of a self-cleaning superhydrophobic surface, the mechanical integrity of the nanoparticle film must be sufficient to withstand wear. The mechanical stability of the dip-coated nanoparticle films was studied by a peel test. Adhesive tape with a pressure-sensitive adhesive (PSA) was applied on the surface and removed from the surface prior to deposition of PFTS because PFTS prevents the adhesion of scotch tape on the surface. The nanoparticle films before and after the peel test were examined by SEM. Figure 4A shows such nanoparticle film after the peel test. In the area highlighted by white square, where the peel test was applied, almost all the nanoparticles were removed from the surface, indicating a rather poor adhesion of the nanoparticles on the NH_2 -SAM. In order to improve the stability and to obtain a stable superhydrophobic surface, the substrates were subjected to a sintering process at high temperature. Sintering was performed under O_2 at $1100\ ^\circ\text{C}$ for 2 h. Figure 4B shows the SEM image of the as-sintered substrate after the peel test. The areas with and without peel test showed an equally dense coverage of nanoparticles, indicating a good stability of the nanoparticle layer. This is attributed to the chemical and thermal bonding of nanoparticle onto the SiO_2 substrates.¹¹ Some tape adhesives were seen on top of the nanoparticles (red ellipsoids in Figure 4B), which refers to a partial adhesive failure between the PSA and the sintered and hydrophilic surface. Lowering the sintering time to 30 min and the sintering temperature to 900 or $1000\ ^\circ\text{C}$ was possible without apparent loss of adhesion improvement. After deposition of PFTS, the static water contact angle was 150° , indicating the formation of a stable superhydrophobic surface on the sintered substrate. After sintering at $1100\ ^\circ\text{C}$ for 30 min, the nanoparticles were only slightly melted onto the substrates (Figure 4C). No obvious deformation was observed. The height profiles of 20 nanoparticles were averaged on samples before and after sintering (Figure 4D), showing that the aspect ratios (height/fwhm) of the nanoparticles before and after sintering were 1.1 and 0.9, respectively.

Because the nanoparticles are transparent in the visible wavelength range, the superhydrophobic nanoparticle films were also prepared on a glass surface, using the dip-coating method. The transparency of the superhydrophobic surface was determined by UV-vis spectroscopy in transmission mode. Figure 5 shows the UV-vis transmittance on an NH_2 -SAM on glass and on a PFTS-functionalized dip-coated nanoparticle film on glass. For

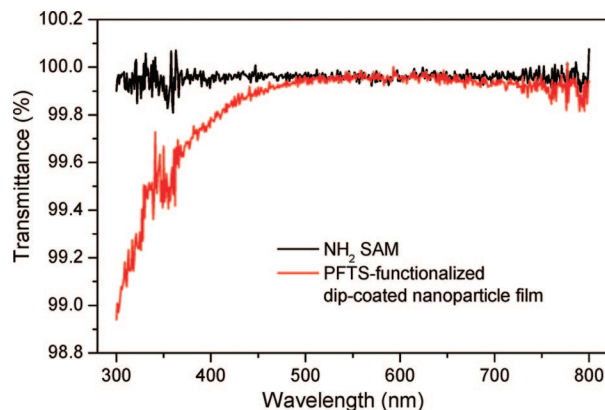


Figure 5. The transmittance of an NH_2 -SAM and of a dip-coated nanoparticle film (both after correction for transmittance of the glass substrates used).



Figure 6. A photograph of water droplets on a superhydrophobic glass surface, prepared by the dip-coating method and functionalization with PFTS.

the NH_2 -SAM on glass, the transmittance was 100% throughout the visible wavelength range. The dip-coated nanoparticle film on glass had also a transmittance of near 100%, but showed some scattering at $\lambda < 500\ \text{nm}$. A photograph of the superhydrophobic surface on glass is shown in Figure 6.

Conclusions

Superhydrophobic surfaces on silicon and glass substrates have been prepared by dip-coating of 60 nm SiO_2 nanoparticles onto an NH_2 -SAM, followed by chemical vapor deposition of PFTS. The nanoparticle film achieved superhydrophobic characteristics ($\theta_w \sim 150^\circ$) because the dip-coating method led to moderate coverage with a high surface roughness. The stability of the superhydrophobic films could be enhanced by sintering of the nanoparticles in an O_2 environment at high temperature. The dip-coating method can be applied on glass surfaces to form superhydrophobic and transparent substrates. Our technique offers a simple and low-cost process to form stable and transparent superhydrophobic surfaces.

Acknowledgment. The Dutch Ministry of Economics Affairs, Province Overijssel, and Province Gelderland are acknowledged for funding of the “Microdruppel” project. We thank Iwan Heskamp, Wilbur de Kruijf, and Jeroen Wissink at Medspray B.V. for the sintering process and useful discussions.